JOURNAL OF MATERIALS SCIENCE 27 (1992) 5269–5275

Spectroscopic characterization of alkali borosilicate glasses containing iron ions

S. MUSIĆ, K. FURIĆ, Z. BAJS, V. MOHAČEK
Ruđer Bošković Institute, P.O. Box 1016, 41001 Zagreb, Republic of Croatia

Structural properties of alkali borosilicate glasses containing iron ions were investigated using infrared, laser Raman and Mössbauer spectroscopy. Two types of glasses were prepared: SRL-type with the composition 18.5 wt% Na_2O, 10.0 wt% B_2O_3, 52.5 wt% SiO_2, 4.0 wt% Li_2O, 10 wt% TiO_2 and 5.0 wt% CaO, and sodium borosilicate glass with the composition 16.7 wt% Na_2O, 18.7 wt% B_2O_3 and 64.6 wt% SiO_2. Raman spectroscopy showed that orthosilicates are the dominant amorphous phase in the SRL-type of glass. Incorporation of iron in the SRL-type of glass induced polymerization of silicate units and –Si–O–Fe– copolymerization. It was concluded that different amorphous phases are simultaneously present in the SRL-type of glass containing iron ions. Interpretation of the Raman spectra is given. Incorporation of iron ions into the sodium borosilicate glass also affected the corresponding IR spectra. The valence state of iron and its coordination were determined by ^{57}Fe Mössbauer spectroscopy.

1. Introduction

In the past 30 years, different oxide glasses have been investigated [1] as possible solidification matrices in the process of immobilization of highly radioactive liquid waste (HRLW). Alkali borosilicate glass possesses several advantages in relation to other oxide glasses which were considered for the immobilization of HRLW, and these advantages can be summarized as follows. Alkali borosilicate glass can easily incorporate almost all of the fission products, while the components that do not dissolve into glass are dispersed as inclusions. It has a high capacity for the nuclear waste oxides and 25–30 wt % of these oxides can be incorporated into the glass matrix. Variations in waste compositions are not critical. Alkali borosilicate glass is characterized by relatively good corrosion resistance in an aqueous medium and it is stable to ionizing radiation. A convenient and compact product can be obtained directly by casting the glass melt in a stainless steel container. Zn–borosilicate and phosphate glasses have also received considerable attention in the past, as possible solidification matrices for the immobilization of HRLW. For practical reasons, very different characterizations (chemical, mechanical, etc.) were performed with simulated nuclear waste glasses. However, the structural properties of these glasses were less investigated. The structure of nuclear waste glasses is of a very complex nature, because they can contain more than 50 elements dissolved in the glass matrix.

Musić *et al.* [2] investigated the effects of iron on the structural properties of Zn–borosilicate and Pb–metaphosphate glasses. Zn–borosilicate glass was prepared with varying amounts of Fe_2O_3, up to 30 wt %. The iron added in the form α-FeOOH, α-Fe_2O_3 or Fe_3O_4, affected the Fe^{3+}/Fe^{2+} ratio, as well as the distribution of iron ions at different coordination sites. At high Fe_2O_3 content, the crystallization of zinc ferrite into the glass matrix was observed. X-ray diffraction and the ^{57}Fe Mössbauer spectroscopy showed that the amount of zinc ferrite in Zn–borosilicate glass decreased in the following order of addition: α-FeOOH → α-Fe_2O_3 → Fe_3O_4. In Pb–metaphosphate glass containing high amounts of Fe_2O_3 the crystallization of $Fe_3(PO_4)_2$ was pronounced.

Musić *et al.* [3] investigated the corrosion of a stainless steel (316L) pot during the melting of Pb–metaphosphate or Pb–Fe–phosphate glass. Different corosion products were identified. The results of the study showed that the corrosion rate of stainless steel in contact with the Pb–metaphosphate or Pb–Fe–phosphate glass melts is high, and due to this fact it was concluded that a stainless steel pot is not suitable for the immobilization of HRLW with phosphate glasses.

The influence of iron ions on the structural properties of Zn–borosilicate glasses was additionally investigated by Musić *et al.* [4]. In the system Na_2O–ZnO–B_2O_3–SiO_2–Fe_2O_3 the presence of only one crystalline phase, $ZnFe_2O_4$, was detected. X-ray diffraction showed that crystallization is more pronounced in the system ZnO–B_2O_3–SiO_2–Fe_2O_3, and in this system the presence of different crystalline phases such as ZnO, γ-Fe_2O_3, Fe_3O_4, $ZnFe_2O_4$ and Fe_3BO_5 was observed. The crystallization of α-Zn_2SiO_4 in the system ZnO–B_2O_3–SiO_2 was confirmed by X-ray diffraction and infrared spectroscopy.

^{57}Fe Mössbauer spectroscopy was used to study the valence state of ions and its coordination in borosilicate glasses [5], which were previously investigated as possible solidification matrices for the immobilization

0022–2461

indicated a strong dependence of the valence state of iron and its coordination on the chemical composition of the glass and the Fe_2O_3 content. It was shown that for a proper chemical composition, Fe^{3+} and/or Fe^{2+} ions may have both types of coordination (IV and VI) at the same time.

Alkali borosilicate glasses of different chemical composition were doped with simulated nuclear waste oxides and the chemical corrosion in water of these glasses was followed by measuring the leach rates (g cm^{-2} day^{-1}), as a function of time [6]. It was found that a simulated nuclear waste glass with the chemical composition 15.61 wt % Na_2O, 10.39 wt % B_2O_3, 45.31 wt % SiO_2, 13.42 wt % ZnO, 6.61 wt % TiO_2 and 8.66 wt % waste oxides is characterized by a relatively low melting temperature and by good corrosion resistance in water. Before the immobilization of HRLW within a glass matrix, HRLW is usually converted to oxide form by direct calcination or chemically treated with organic reducers, for instance with formic acid [7].

Recently, Musić *et al.* [8] showed the usefulness of laser Raman spectroscopy in the study of the structural properties of sodium borosilicate glass containing different foreign cations. In continuation of this work [8], we report the results of the investigation of the structural properties of alkali borosilicate glasses using spectroscopic techniques, such as Raman, infrared and Mössbauer spectroscopy. The emphasis was on the alkali borosilicate glass, which was investigated some years ago as a possible matrix for the immobilization of HRLW at the Savannah River Laboratories, Aiken, South Carolina [9].

2. Experimental procedure

All chemicals were A.R. grade. Chemicals were in the form of carbonate or oxide. Amorphous SiO_2 (precipitated) was prepared using the procedure given by Filipović-Vinceković and Musić [10].

Glass samples were prepared using the following procedure. Appropriate amounts of the corresponding chemicals in the powdered state were mixed. A small amount of doubly distilled water was added to this mixture and after homogenization the mixture was dried. The glass was melted in contact with the air. A new crucible was used for the preparation of each sample. The crucibles were made from ceramic material with a low corrosion rate at high temperatures. In several cases, stainless steel crucibles were also used. The temperature in the furnace was increased gradually to prevent uncontrolled foaming. The molten glass was poured into a graphite mould which was preheated in the furnace to prevent abrupt cooling and cracking of the glass. The glass melt was slowly cooled to room temperature.

Glasses were crushed to powder form for Mössbauer and infrared spectroscopic measurements. For laser Raman spectroscopy, glass samples were cut into small cubes and optically polished.

The infrared spectra were recorded with a 580B Perkin–Elmer spectrometer. The glass powder was pressed in a KBr disc.

through standard geometry at 90°. A coherent Innova – 100 laser with $\lambda_0 = 514.5$ nm served as an excitation source and the scattered light was analysed using a DILOR Z-24 Raman spectrometer. Typical laser power at the sample was 500 mW. Spectra were recorded in sequential mode with the spectral slitwidth ≈ 2 cm^{-1} and the accumulation time of 1 s. Only in the case of the darkest sample (S-5) was multiscanning with four scans performed.

^{57}Fe Mössbauer spectra were recorded using a spectrometer produced by Wissel (D-8130 Starnberg, FRG). A $^{57}Co/Rh$ source (Amersham) was used.

All spectra were recorded at room temperature.

3. Results and discussion

Fig. 1 shows the infrared spectrum of amorphous SiO_2 (sample S-1), which was used in the present work as a starting component for the preparation of glasses. The main characteristics of this spectrum are the dominant band at 470 cm^{-1} with a shoulder at $\sim$ 550–600 cm^{-1} and bands at 800 and 900 cm^{-1}. A broad band is also visible in the region of higher wave numbers with a transmission minimum at 1090 cm^{-1} and a shoulder at $\sim$ 1200 cm^{-1}.

Bock and Gouq-Jen Su [11] made a comparison of observed and calculated vibrational spectra for vitreous silica. The infrared spectrum recorded for vitreous silica was characterized with bands at 377, 465, 800, 950, 1100 and 1190 cm^{-1}.

The infrared spectrum of amorphous SiO_2 with transmission minima near 460, 800 and 1075 cm^{-1} is very similar to that of crystalline quartz (α-SiO_2) with the main difference being a general increase in the width of the infrared bands [12]. The band at 1075 cm^{-1} was traditionally interpreted as the Si–O bond stretching mode. Boyd [13] deconvoluted the band at 1075 cm^{-1} into two peaks with Gaussian profile. The derived peaks were found to be at 1050 cm^{-1} with a full width half-maximum transmission value (FWHM) of 65 cm^{-1}, and at 1085 cm^{-1} with a FWHM of 35 cm^{-1}. This observation was ascribed to at least two structures existing in amorphous SiO_2.

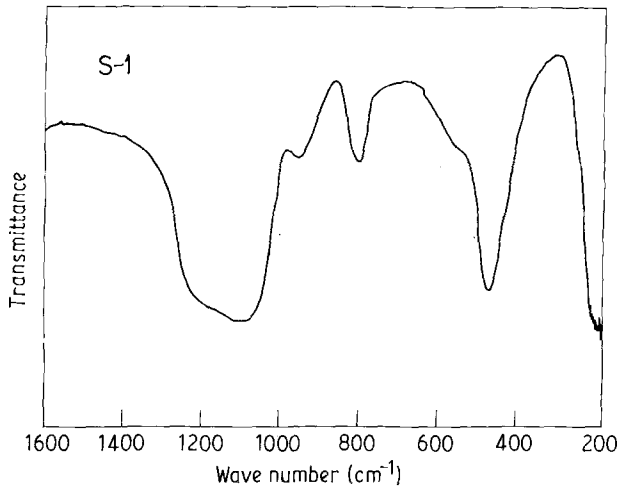

Figure 1 Infrared spectrum of amorphous SiO_2 (precipitated).

Silica and orthosilicates are often used as references in the study of silicate glasses. The structure of silica can be expressed as the polymerized arrangement of SiO_4^{4-} tetrahedral units contrary to the orthosilicates which can be expressed by the isolated SiO_4^{4-} ions. Ferraro *et al.* [14] studied the nature of silicate glasses using infrared spectroscopy. Physical interpretation of different infrared bands is presented.

White and Minser [15] found that the Raman spectra of natural silicate glasses were very similar to those obtained for synthetic glasses with the same chemical composition. It was observed that Raman spectra were characterized with two dominant regions, 800–1200 cm^{-1}, 400–650 cm^{-1} and a region below 300 cm^{-1}. The 800–1200 cm^{-1} region may show one to three highly polarized bands associated with the symmetric stretching motions of silica tetrahedra containing one to four non-bridging oxygens (NBO). The 400–650 cm^{-1} region usually shows one intense polarized band which can be accompanied by several weak peaks. Raman spectra of silicate glasses show an intense depolarized band, called a boson peak, in the range 50–100 cm^{-1}, the intensity of which changes rapidly with temperature. Malinovsky *et al.* [16] found that the spectral form of the boson peak is the same for different oxide, chalcogenide or organic glasses.

Fig. 2 shows Raman spectra of samples S-2, S-3, S-4 and S-5 recorded at room temperature. The chemical composition of glass S-2 is 18.5 wt % Na_2O, 10.0 wt % B_2O_3, 52.5 wt % SiO_2, 4.0 wt % Li_2O, 10.0 wt % TiO_2 and 5.0 wt % CaO. Glasses S-3, S-4 and S-5 were prepared by adding 5, 10 and 20 wt % α-Fe_2O_3 to the chemical composition of glass S-2. The melting of these glasses was performed in a ceramic melter.

The main characteristic of spectrum S-2 is a very strong and broad peak at 882 cm^{-1}. Three peaks of medium intensity are located at 1062, 538 and 318 cm^{-1}. Two weak peaks are also observed at 694 and 630 cm^{-1}. The peak position of the boson peak is at 102 cm^{-1}.

Fig. 3 shows VH polarized Raman spectra of samples S-2, S-3, S-4 and S-5 at room temperature, and in Fig. 4 the VV polarized Raman spectra of the same samples are presented.

A Raman spectrum similar to the spectrum of our sample S-2 was recorded for SRL glass Frit 21A by Sales *et al.* (see Fig. 7. in [17]). The chemical composition of glass Frit 21A is 55.2 wt % SiO_2, 10.5 wt % B_2O_3, 19.5 wt % Na_2O, 10.5 wt % TiO_2 and 4.3 wt % Li_2O. Sales *et al.* [17] ascribed a large peak at 870 cm^{-1} to Ti–O vibrations and a shoulder at 1046 cm^{-1} to non-bridging oxygen bonds. The Raman spectrum of Frit 21A + 5 wt % SiO_2 was essentially the same as the Raman spectrum of Frit 21A.

We interpret the Raman spectrum of sample S-2 shown in Fig. 2 in the sense of the orthosilicates present as the dominant amorphous phase in the glass. A very strong and broad peak at 882 cm^{-1} can be ascribed to the superposition of ν_1 and ν_3 frequencies of the orthosilicate unit. This conclusion is confirmed after the recording of the spectrum of sample S-2 in different polarizations. Fig. 3 shows an intense peak at 920 cm^{-1} for sample S-2, while Fig. 4 shows an intense peak at 874 cm^{-1}. Peaks at 538 and 318 cm^{-1} can be ascribed to ν_4 and ν_2 frequencies of the orthosilicate unit and this conclusion is also supported by polarized Raman spectra. The peak of small intensity at 630 cm^{-1} (Fig. 2) is probably due to the presence of the ring-type metaborate group which has characteristic band at 630 cm^{-1}. A very weak peak at

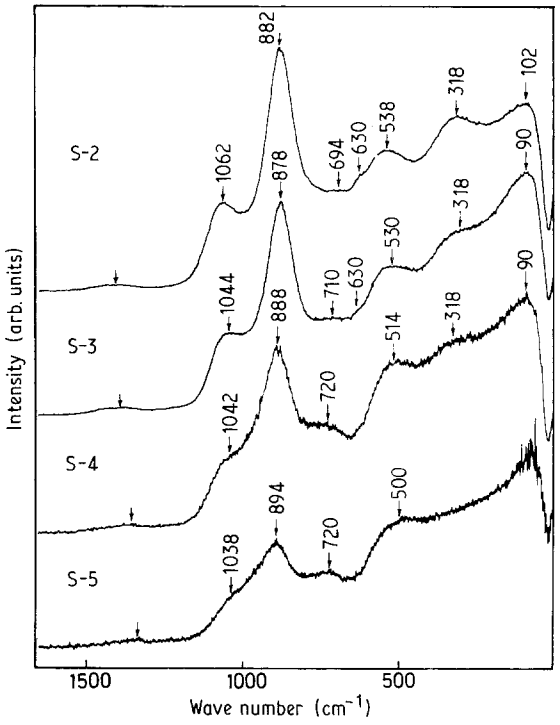

Figure 2 VV polarized Raman spectra of SRL-type of glass (sample S-2), with different amounts of Fe_2O_3. Sample S-3 contains 5 wt % Fe_2O_3, sample S-4 10 wt % Fe_2O_3, and sample S-5 20 wt % Fe_2O_3.

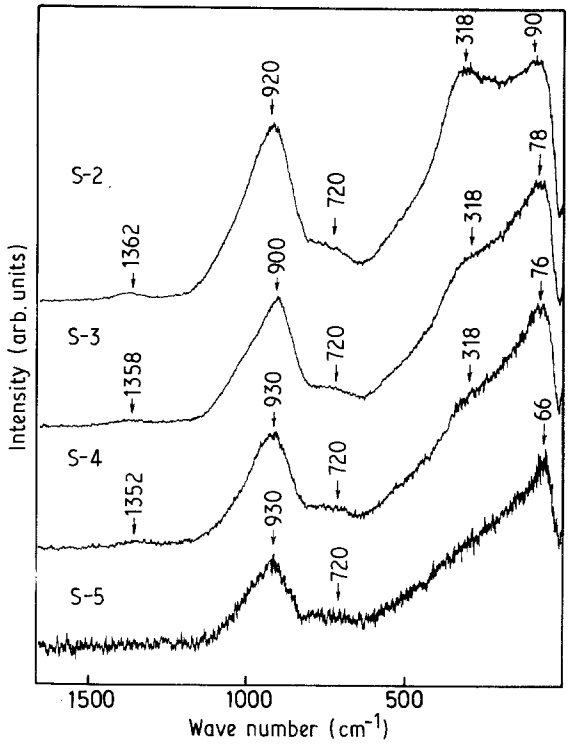

Figure 3 VH polarized Raman spectra of samples S-2, S-3, S-4 and S-5.

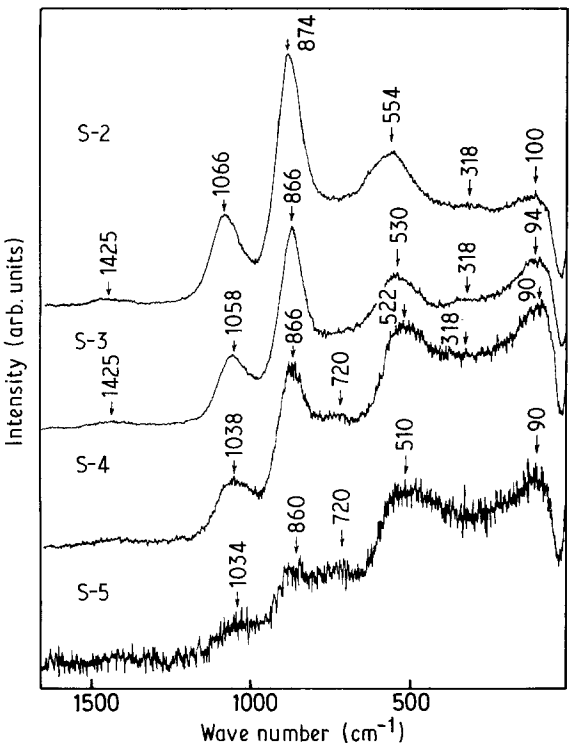

Figure 4 VV – (4/3) VH polarized Raman spectra of samples S-2, S-3, S-4 and S-5.

$\sim 1430\ cm^{-1}$ is sometimes interpreted in terms of the presence of carbonate group [18].

Incorporation of iron ions into the structure of glass S-2 significantly affects the corresponding Raman spectra. The intensity of the peak at $318\ cm^{-1}$ decreases with the increasing iron content and this peak does not become more visible in the spectrum of sample S-5. The intensity of the peak at $538\ cm^{-1}$ also decreases with increasing iron content and shifts to $500\ cm^{-1}$ for sample S-5. For the same chemical compositions, the relative intensity of a very strong band at $882\ cm^{-1}$ also decreases with increasing iron content and the peak at $1062\ cm^{-1}$ becomes a shoulder at $1038\ cm^{-1}$ in the spectrum of sample S-5. The weak peak at $694\ cm^{-1}$ shifts to $720\ cm^{-1}$. The origin of this peak was discussed in our previous paper [8], and the effect observed indicates the tendency of dimerization of isolated silicate units. Other effects, such as the decrease of relative intensity and pronounced broadening of the peak at $882\ cm^{-1}$, a shoulder at $1038\ cm^{-1}$ and the presence of a peak at $500\ cm^{-1}$, indicate "repairing" of the silicate (borosilicate) network in the sense of the incorporation of iron in the polymers (copolymerization –Si–O–Fe–) and the tendency of polymerization of isolated silicate units. It can be concluded that very probably different amorphous phases are present simultaneously in the glass of the SRL (Savannah River Laboratories) composition.

Our conclusions, based on the laser Raman spectroscopy, can be supported by the results of other researchers in the field of vibrational spectroscopy of silicate and borosilicate glasses. For instance, Konijnendijk and Stevels [19] investigated the molecular structure of borosilicate glasses also using Raman spectroscopy. It was shown that the same type of groups are present in borosilicate glasses as in borate and silicate glasses. Peak positions of the Raman bands (approximately) of borate groups and silicate units are shown in Table I.

Husung and Doremus [20] studied infrared spectra of different silicate glasses in the form of blown films. The authors assigned the infrared bands for a blown film of the Pyrex composition, as shown in Table II.

Kamitsos *et al.* [21] found that Raman spectroscopy is very effective in the investigation of the formation of non-bridging oxygen (NBO) containing pyro- and metaborate units. On the other hand, infrared spectroscopy clearly followed the destruction of diborate groups and the formation of boroxol rings, but gave no clear answer as to the nature of the NBO-containing borate groups. Table III shows assignments of the Raman bands present in the spectra $xMgO \cdot yNa_2O \cdot B_2O_3$ glasses to specific borate groups.

Piriou and McMillan [22] studied vibrational spectra of some vitreous and crystalline orthosilicates. A strong polarized band at $854\ cm^{-1}$, observed for $CaMgSiO_4$ glass, was ascribed to the ν_1 vibration of an isolated SiO_4 unit, and its depolarized high-frequency shoulder mainly to ν_3 vibration. The weak double bond at 520–600 cm^{-1} in the $CaMgSiO_4$ glass was partially assigned to the asymmetric deformation, ν_4, of the SiO_4 tetrahedron.

The vitreous fayalite, Fe_2SiO_4, showed three infrared bands at $933\ cm^{-1}$ (very strong), $695\ cm^{-1}$

TABLE I Approximate Raman peak positions of borate groups and silicate units [19]

Peak position (cm^{-1})	Origin
435, 495	SiO_4 tetrahedra with four bridging oxygen ions
540	SiO_4 tetrahedra with one non-bridging oxygen ion
590	SiO_4 tetrahedra with two non-bridging oxygen ions
630	Ring-type metaborate groups
760	Six-membered ring with two BO_4 tetrahedra
770	Six-membered borate ring with one BO_4 tetrahedron
806	Boroxol group
950	SiO_4 tetrahedra with two non-bridging oxygen ions
1090	SiO_4 tetrahedra with one non-bridging oxygen ion

TABLE II Assignation of the infrared bands for a blown film of the Pyrex composition [20]

Infrared band (cm^{-1})	Assignation
1390	B–O stretching
1080	Si–O stretching (within tetrahedra)
920	B–O–Si stretching
805	Si–O–Si stretching (between tetrahedra)
680	B–O–Si stretching
460	Si–O–Si and O–Si–O bending

TABLE III Assignments of the Raman bands of specific borate groups present in the spectra of $xMgO \cdot yNa_2O \cdot B_2O_3$ glasses [21]

Peak position (cm^{-1})	Assignation
1430–1500	B–O–bonds attached to large borate groups
1285–1290	Pyroborate units
1120	Diborate groups
930–945	Orthoborate units
840–850	Pyroborate units
805	Boroxol rings
780–785	Six-membered rings with one BO_4 (e.g. tri-, tetra-, or pentaborate groups)
760	Six-membered ring with two BO_4's (e.g. di-tri-, di-pentaborate groups)
630–690	Ring and/or chain type metaborate units
490–570	"Isolated" diborate units

(very weak) and 508 cm^{-1} (strong), which were assigned to the Fe_2 antisymmetric stretching mode ν_3, the A_1 total symmetric stretching mode, ν_1, and the Fe_2 bending mode, ν_4, of the SiO_4 unit, respectively [23].

Williams *et al.* [24] investigated vibrational spectra of olivine glasses, Mg_2SiO_4 and Mn_2SiO_4. The parallel-polarized (VV) Raman spectrum of Mg_2SiO_4 is dominated by a strong polarized band at 864 cm^{-1}. This band is asymmetric on its high-frequency side, due to the presence of a broad depolarized band present in the perpendicularly polarized (VH) spectrum near 900 cm^{-1}. These polarized and depolarized Raman bands were ascribed to ν_1 (symmetric) and ν_3 (asymmetric) stretching vibrations of tetrahedral SiO_4 units in the glass structure. The high-frequency maximum in the infrared spectrum at 979 cm^{-1} is also due to the ν_3 vibration of tetrahedral SiO_4 units. Weak depolarized Raman bands, observed for Mg_2SiO_4 near 520 and 330 cm^{-1}, were assigned to ν_4 and ν_2 frequencies and/or vibrations of magnesium polyhedra. The location of an infrared band at 720 cm^{-1} corresponds well with that ascribed to symmetric stretching of bridging oxygen atoms in Si_2O_7 groups in both glassy and crystalline silicates. The band at 625 cm^{-1} is probably due to the bridging oxygen vibrations of highly polymerized silicate species within the glass.

Cooney and Sharma [25] used Raman spectroscopy to study structural properties of orthosilicate glasses in the systems Mg_2SiO_4–Fe_2SiO_4, Mn_2SiO_4–Fe_2SiO_4, Mg_2SiO_4–$CaMgSiO_4$ and Mn_2SiO_4–$CaMnSiO_4$. Raman spectra of Mg_2SiO_4, Fe_2SiO_4 and Mn_2SiO_4 glasses are characterized by a strong polarized band at 840–870 cm^{-1} containing an asymmetric partially depolarized band near 900 cm^{-1}. A weak band at 625–725 cm^{-1} is also observed. Mg_2SiO_4 glass showed the ν_1 band position at 869 cm^{-1} and for Mg_2SiO_4 crystal at 856 cm^{-1}. This difference in the position of ν_1 band was explained by the difference in the Si–O vibrations in two states, amorphous versus crystalline. The low-intensity band at 700 cm^{-1} in both Raman and infrared spectra was interpreted as symmetric stretching vibrations of bridging oxygens in Si_2O_7 dimers. It was suggested that Mg^{2+} and Ca^{2+} behave as network modifiers, while Fe^{2+} ions serve as network forming and charge balancing cations.

Fig. 5 shows the Mössbauer spectra of samples S-3 and S-5 recorded at room temperature. The Mössbauer spectrum of sample S-3 is characterized by a quadrupole doublet, which can be supposed to be a superposition of two doublets, Q_1 and Q_2. Their parameters are: $\delta_1 = 0.29\ mm\ s^{-1}$, $\Delta_1 = 0.98\ mm\ s^{-1}$, $\delta_2 = 0.26\ mm\ s^{-1}$ and $\Delta_2 = 1.32\ mm\ s^{-1}$. The Mössbauer spectrum of sample S-5 is characterized by a quadrupole doublet and the corresponding parameters $\delta_1 = 0.29\ mm\ s^{-1}$ and $\Delta_1 = 0.98\ mm\ s^{-1}$. Generally, the isomer shift, δ, for Fe^{3+} at tetrahedral site is smaller than that for Fe^{3+} at the octahedral site. In many cases the values of isomer shift for both coordination sites overlap, and for this reason it is better to use the value of quadrupole splitting as a measure of the iron ion coordination in oxide glasses. It can be supposed that $\Delta_1 = 0.98\ mm\ s^{-1}$ corresponds to Fe^{3+} in tetrahedral or very deformed octahedral symmetry. $\Delta_2 = 1.32\ mm\ s^{-1}$ can be ascribed to Fe^{3+} ions at tetrahedral sites. Musić [5] showed that determination of the iron state in oxide glasses is not a simple problem. For a certain chemical composition iron can be present in the form of Fe^{3+} and/or Fe^{2+} ions occupying both the tetrahedral and octahedral sites. However, many researchers used a formalistic approach in the determination of iron ion coordination supposing that iron ions substitute tetrahedral Si^{4+} and that for this reason all iron ions must also be at tetrahedral sites.

Darby Dyar [26] and Tomandl [27] reviewed the application of Mössbauer spectroscopy in the determination of the valence state and coordination of iron in oxide glasses.

Nishida *et al.* [28] used Mössbauer spectroscopy to study non-bridging oxygen atoms in potassium borosilicate glasses. Mössbauer parameters for glasses

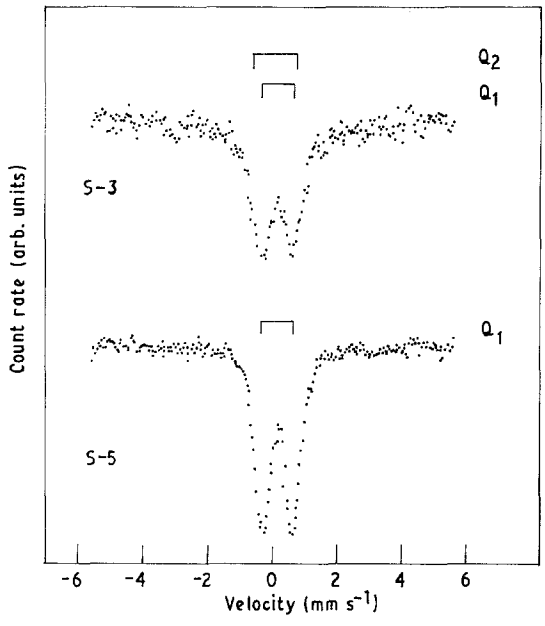

Figure 5 ^{57}Fe Mössbauer spectra of samples S-3 and S-5, recorded at room temperature.

$xK_2O \cdot (100 - x)(B_2O_3, SiO_2) \cdot 7Fe_2O_3$, where $SiO_2/B_2O_3 = 2$, changed for δ_{Fe} from 0.31 mm s^{-1} to 0.22 mm s^{-1} and for Δ from 1.03 mm s^{-1} to 0.78 mm s^{-1}, when x changed from 12 mol % to 40 mol %. It was concluded that all iron is present in the form of Fe^{3+} ions with tetrahedral symmetry.

Hirao *et al.* [29] recorded Mössbauer spectra at room temperature for sodium silicate glasses and crystals containing 3–15 mol % Fe_2O_3. They concluded that iron ions in silicate glasses are mainly at tetrahedral sites, when the iron content is high. It was also suggested that a large number of nonidentical sites exist in iron–sodium–silicate glasses than in the corresponding crystals.

Mössbauer spectroscopy was used to follow gel–glass transformation in the system SiO_2–Fe_2O_3 containing 5–40 wt % Fe_2O_3 [30]. Iron silicate glasses with all the iron ions present as Fe^{3+} were obtainable by the gel route, whereas simple melting of oxides failed to produce them. The coordination of Fe^{3+} ions was determined as tetrahedral.

Fig. 6 shows the infrared spectra of samples S-6, S-7 and S-8. The chemical composition of these glasses is 16.7 wt % Na_2O, 18.7 wt % B_2O_3 and 64.5 wt % SiO_2. Sample S-6 was melted for 1 h at 1100 °C, sample S-7 was melted for 30 min at 1100 °C and sample S-8 was melted for 2 h at 1000 °C. Fig. 6 does not show differences in the corresponding infrared spectra of samples S-6, S-7 and S-8. The Raman spectrum of this glass and peak assignations were discussed in our previous paper [8]. In the infrared spectrum three main bands, typical for sodium borosilicate glass, are observed near 470, 1010 and 1410 cm^{-1} with shoulders at 710 and 800 cm^{-1}.

The addition of iron to sodium borosilicate glass affects the corresponding infrared spectrum. Fig. 7 shows the infrared spectra of samples S-9, S-10 and S-11. These samples were prepared by adding different amounts of α-Fe_2O_3 (5, 15 or 30 wt %) to sodium borosilicate glass (S-6 composition). These samples were completely amorphous, as determined by X-ray diffraction.

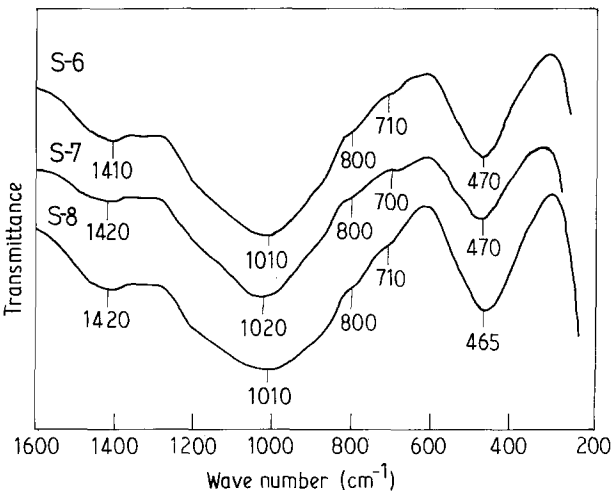

Figure 6 Infrared spectra of sodium borosilicate glass prepared with different melting times (sample, S-6, 1 h at 1100 °C; sample S-7 30 min at 1100 °C and sample S-8 2 h at 1000 °C.

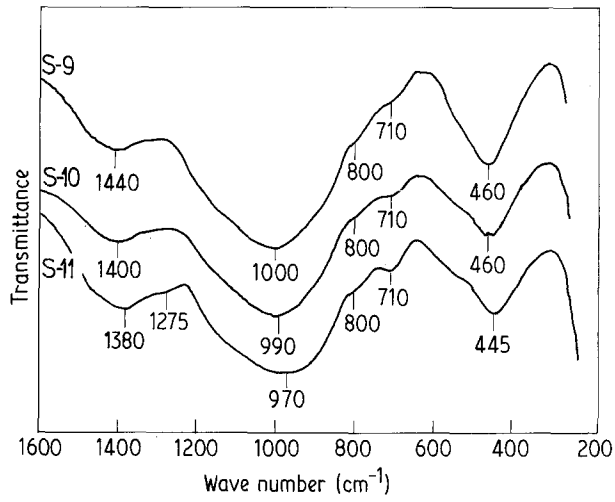

Figure 7 Infrared spectra of sodium borosilicate glass containing different amounts of Fe_2O_3. Sample S-9 contains 5 wt % Fe_2O_3, sample S-10 10 wt % Fe_2O_3, and sample S-11 30 wt % Fe_2O_3.

Incorporation of iron ions into sodium borosilicate glass generated the following change in the infrared spectrum. The infrared band at 470 cm^{-1} was additionally broadened and shifted to 445 cm^{-1} with increasing iron content. In the infrared spectrum of sample S-11 a shoulder at 550 cm^{-1} appeared. The broad infrared band at 1000 cm^{-1} is shifted to 970 cm^{-1}, and the broad band at 1410 cm^{-1} is shifted to 1380 cm^{-1}. In the same spectrum of S-11, a weak band at 1275 cm^{-1} is also visible. The shoulder at 800 cm^{-1} did not change its intensity and position, but the shoulder at 710 cm^{-1} transformed to a peak at the same position on increasing the iron content.

Particular attention was paid to the peak at 710 cm^{-1}, as in our previous work [8], where the same effect was observed for sodium borosilicate glass containing Eu^{3+}. This effect can be interpreted as a result of the incorporation of Fe^{3+} or generally Me^{3+}, where Me is the metal, into the network of the oxide glasses. The infrared band near 700 cm^{-1} is characteristic of $NaAlO_2$ or $Ca_{0.5}AlO_2$ substitution of the silicate network in numerous aluminosilicate glasses, where Al/(Al + Si) exceeds ≈ 0.25 [18]. This infrared band near 700 cm^{-1} can be used as a good indication of the presence of network-substituted AlO_4 polyhedra, which is consistent with the study of Tarte [31].

Fig. 8 shows ^{57}Fe Mössbauer spectra of samples S-9, S-10 and S-11. Mössbauer spectra of samples S-9, S-10 indicate the presence of Fe^{3+} and 15%–20% Fe^{2+}, while Mössbauer spectrum of sample S-11 indicates only the presence of Fe^{3+}. The spectral lines are not sharp, thus indicating non-equivalent environments around iron ions, i.e. the structural sites are not well defined as in crystals. The values of isomer shift and quadrupole splitting are the following. For sample S-9, $\delta_1 = 0.24$ mm s^{-1}, $\Delta_1 = 0.88$ mm s^{-1}, $\delta_2 = 0.26$ mm s^{-1}, $\Delta_2 = 1.32$ mm s^{-1}, $\delta_3 = 0.97$ mm s^{-1} and $\Delta_3 = 2.40$ mm s^{-1}, for sample S-10, $\delta_1 = 0.31$ mm s^{-1}, $\Delta_1 = 0.93$ mm s^{-1}, $\delta_2 = 1.00$ mm s^{-1} and $\Delta_2 = 2.40$ mm s^{-1} and for sample S-11, $\delta_1 = 0.29$ mm s^{-1} and $\Delta_1 = 1.00$ mm s^{-1}. Mössbauer parameters, δ and Δ, recorded for Fe^{2+} ions in samples S-9 and S-10 can be

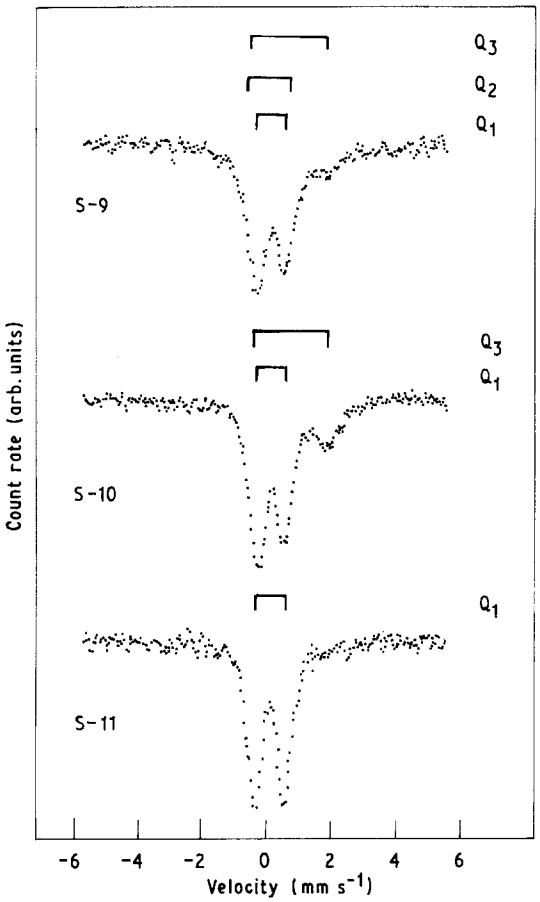

Figure 8 ^{57}Fe Mössbauer spectra of samples S-9, S-10 and S-11, recorded at room temperature.

ascribed to Fe^{2+}_{tet}, while the coordination of Fe^{3+} can be interpreted in a similar way as for SRL-type of glass.

Acknowledgements

We thank Professor S. Popović for XRD measurements and Mr J. Forić for technical assistance.

References

1. C. M. JANTZEN, *J. Non-Cryst. Solids* **84** (1986) 215.
2. S. MUSIĆ, M. GOTIĆ, S. POPOVIĆ and B. GRŽETA, *J. Radioanal. Nucl. Chem.* **116** (1987) 141.
3. S. MUSIĆ, M. GOTIĆ and S. POPOVIĆ, *J. Mater. Sci. Lett.* **8** (1989) 1389.
4. S. MUSIĆ, S. POPOVIĆ and M. GOTIĆ, *J. Radioanal. Nucl. Chem.* **130** (1989) 299.
5. S. MUSIC, *J. Mater. Sci. Lett.* **8** (1989) 537.
6. S. MUSIĆ, M. RISTIC, M. GOTIĆ and J. FORIĆ, *J. Radioanal. Nucl. Chem.* **122** (1988) 91.
7. S. MUSIĆ, M. RISTIĆ and S. POPOVIĆ, *ibid.* **134** (1989) 353.
8. S. MUSIĆ, Z. BAJS, K. FURIĆ and V. MOHAČEK, *J. Mater. Sci. Lett.* **10** (1991) 889.
9. R. P. SCHUMAN, N. D. COX, G. W. GIBSON and P. V. KELSEY Jr, Evaluation of forms for the immobilization of high-level and transuranic wastes, Report EGG-FM-6045, EG&G Idaho Inc., August 1982, Idaho Falls, ID 83415.
10. N. FILIPOVIĆ-VINCEKOVIĆ and S. MUSIĆ, unpublished results.
11. J. BOCK and GOUQ-JEN SU, *J. Amer. Chem. Soc.* **53** (1970) 69.
12. P. H. GASKELL and D. W. JOHNSON, *J. Non-Cryst. Solids* **20** (1976) 153.
13. I. W. BOYD, *Appl. Phys. Lett.* **51** (1987) 418.
14. J. W. FERRARO, M. H. MANGHNANI and A. QUATROCHI, *Phys. Chem. Glasses* **13** (1972) 116.
15. W. B. WHITE and D. G. MINSER, *J. Non-Cryst. Solids* **67** (1984) 45.
16. V. K. MALINOVSKY, V. N. NOVIKOV and A. P. SOKOLOV, *ibid.* **90** (1987) 485.
17. B. C. SALES, C. W. WHITE, G. M. BEGUN and L. A. BOATNER, *ibid.* **67** (1984) 245.
18. W. R. TAYLOR, *Proc. Indian Acad. Sci. (Earth Planet Sci.)* **99** (1990) 99.
19. W. L. KONIJNENDIJK and J. M. STEVELS, *J. Non-Cryst. Solids* **20** (1976) 193.
20. R. D. HUSUNG and R. H. DOREMUS, *J. Mater. Res.* **5** (1990) 2209.
21. E. I. KAMITSOS, M. A. KARAKASSIDES and G. D. CHRYSSIKOS, *J. Phys. Chem.* **91** (1987) 1073.
22. B. PIRIOU and P. McMILLAN, *Amer. Mineral.* **68** (1983) 424.
23. K. KUSABIRAKI and Y. SHIRASHI, *J. Non-Cryst. Solids* **44** (1981) 365.
24. Q. WILLIAMS, P. McMILLAN and T. F. COONEY, *Phys. Chem. Minerals* **16** (1989) 352.
25. T. F. COONEY and S. K. SHARMA, *J. Non-Cryst. Solids* **122** (1990) 10.
26. M. DARBY DYAR, *Amer. Mineral.* **70** (1985) 304.
27. G. TOMANDL, "Mössbauer Effect in Glasses", in "Glass: Science and Technology", Vol. 48 (Academic Press, 1990) p. 273.
28. T. NISHIDA, T. HIRAI and Y. TAKASHIMA, *Phys. Chem. Glasses* **22** (1981) 94.
29. K. HIRAO, T. KOMATSU and N. SOGA, *J. Non-Cryst. Solids* **40** (1980) 315.
30. M. GUGLIELMI and G. PRINCIPI, *ibid.* **48** (1982) 161.
31. P. TARTE, *Spectrochim. Acta* **A23** (1967) 2127.

Received 10 June
and accepted 28 October 1991